Cerebral Cortex February 2006;16:149-161
doi:10.1093/cercor/bhi089
Advance Access publication April 27, 2005

Motor control in basal ganglia circuits using fMRI and brain atlas approaches

Stéphane Lehéricy[1], Eric Bardinet[2], Leon Tremblay[3], Pierre-Francois Van de Moortele[1], Jean-Baptiste Pochon[4], Didier Dormont[2], Dae-Shik Kim[5], Jerome Yelnik[3] and Kamil Ugurbil[1]

[1]CMRR/University of Minnesota, Minneapolis, MN, USA, [2]CNRS UPR640, Paris, France, [3]INSERM U289, CHU Salpêtrière, Paris, France, [4]Center for the Study of Brain, Mind and Behavior Princeton University, Princeton, NJ, USA and [5]Department of Anatomy and Neurobiology, Boston University School of Medicine, Boston, MA, USA

In this study, we examined how the motor, premotor and associative basal ganglia territories process movement parameters such as the complexity and the frequency of movement. Twelve right-handed volunteers were studied using EPI BOLD contrast (3 T) while performing audio-paced finger tapping tasks designed to differentiate basal ganglia territories. Tasks varied movement complexity (repetitive index tapping, simple sequence of finger movements and complex sequence of 10 moves) and frequency (from 0.5 to 3 Hz). Activation maps were coregistered onto a 3-D brain atlas derived from post-mortem brains. Three main patterns of activation were observed. In the posterior putamen and the sensorimotor cortex, signal increased with movement frequency but not with movement complexity. In premotor areas, the anterior putamen and the ventral posterolateral thalamus, signal increased regularly with increasing movement frequency and complexity. In rostral frontal areas, the caudate nucleus, the subthalamic nucleus and the ventral anterior/ventrolateral thalamus, signal increased mainly during the complex task and the high frequency task (3 Hz). These data show the different roles of motor, premotor and associative basal ganglia circuits in the processing of motor-related operations and suggest that activation can be precisely located within the entire circuitry of the basal ganglia.

Keywords: basal ganglia, globus pallidus, motor system, movement frequency, subthalamic nucleus

Introduction

In this study, we examined how the motor, premotor and associative basal ganglia territories process parameters such as the complexity and the frequency of movement. Models of basal ganglia organization suggest that they process information in several segregated loops (Alexander *et al.*, 1986; Middleton and Strick, 2000). In monkeys, studies using retrograde transneuronal transport have suggested that one main characteristic of basal ganglia connectivity is characterized by a closed-loop organization, e.g. projections from one area of the cortex innervate areas of the basal ganglia, which project back to the same cortical area (Middleton and Strick, 2000). Electrophysiological studies have also shown many functional similarities between basal ganglia and cortical areas to which they are connected, suggesting that a similar activation pattern may be expected in cortical and related basal ganglia areas (Alexander and Crutcher, 1990; Romo *et al.*, 1992; Schultz *et al.*, 2000). Imaging studies in humans have shown that frontal cortical areas participate differentially in the control of movement. The sensorimotor cortex (SMC) has been identified as an executive area whose activation correlated with basic movement parameters such as frequency (Rao *et al.*, 1996; Sadato *et al.*, 1996b; Jenkins *et al.*, 1997; Wexler *et al.*, 1997; Kawashima *et al.*, 1999) and increased with the number of fingers used to perform the movement (Catalan *et al.*, 1998; Hlustik *et al.*, 2001). In contrast, activation in the SMC did not increase with the complexity of sequences of contralateral finger movements (Sadato *et al.*, 1996a; Boecker *et al.*, 1998; Catalan *et al.*, 1998; Gordon *et al.*, 1998; Harrington *et al.*, 2000). Sequential movements recruited premotor areas (Orgogozo and Larsen, 1979; Roland *et al.*, 1982; Colebatch *et al.*, 1991; Rao *et al.*, 1993; Shibasaki *et al.*, 1993; Sadato *et al.*, 1996a; Jueptner *et al.*, 1997b; Boecker *et al.*, 1998; Catalan *et al.*, 1998; Gordon *et al.*, 1998; Harrington *et al.*, 2000). Activation in premotor areas also correlated with movement frequency (Jenkins *et al.*, 1997). By contrast, the prefrontal cortex was recruited when tasks required higher order motor processes, such as working memory or explicit learning (Jueptner *et al.*, 1997b; Rowe *et al.*, 2000; Wu *et al.*, 2004), and activation was not modulated by basic movement parameters (Jenkins *et al.*, 1997).

Basal ganglia activation was inconsistently observed in functional imaging studies in humans. One report found no correlation between activation and movement frequency in the putamen (Jenkins *et al.*, 1997). Performance of simple repetitive movements (Lehéricy *et al.*, 1998; Maillard *et al.*, 2000) and a well-learned sequence of finger movements (Roland *et al.*, 1982; Shibasaki *et al.*, 1993; Jenkins *et al.*, 1994; Jueptner *et al.*, 1997a) was associated with activation in the putamen. Sequential movement activated the striatum more than non-sequential typing movements (Gordon *et al.*, 1998), and activation in the anterior globus pallidus correlated with increasing sequence length (Boecker *et al.*, 1998). In contrast, some studies did not report any basal ganglia regions specifically related to sequential movements (Shibasaki *et al.*, 1993; Sadato *et al.*, 1996a; Catalan *et al.*, 1998; Harrington *et al.*, 2000). Higher-order motor components, such as explicit learning (Jueptner *et al.*, 1997a), working memory and movement selection tasks (Pochon *et al.*, 2001; Gerardin *et al.*, 2004), recruited more rostral regions of the striatum.

Moreover, to date, the most convincing data were obtained in the striatum. The subthalamic nucleus (STN), which is part of the indirect cortico-basal ganglia circuit, plays an important integrative role in information processing in the indirect circuit (Georgopoulos *et al.*, 1983; DeLong *et al.*, 1985; Penney and Young, 1986; Wichmann *et al.*, 1994; Mink, 1996; Nambu *et al.*, 2000). The STN is involved in the pathophysiology of movement disorders such as Parkinson's disease, and its electrical stimulation is an efficient treatment for this disease (Krack *et al.*, 2003). In spite of its crucial position in motor circuitry, the influence of the STN on motor control is not clear. One reason is that the STN, due to its small size, was beyond functional imaging capacities in humans.

Imaging the basal ganglia is technically challenging because: (i) task-induced signal changes in the basal ganglia are lower than in the cortex; (ii) ferromagnetic particles deposit normally over time in the basal ganglia, particularly in the globus pallidus, the substantia nigra (SN) and the STN, leading to reduced T_2* and signal intensity in functional magnetic resonance (MR) images; (iii) some structures, and particularly the STN, are small, deep nuclei, whose precise location can vary in individuals; and (iv) the STN and the nuclei of the thalamus, the main output structure of basal ganglia efferents, are usually not visible in conventional MR images, which renders their localization more difficult. In this study, we used high-resolution functional magnetic resonance imaging (fMRI) with a high-level magnetic field (3 T) to detect activation in the all basal ganglia nuclei, as well as the thalamic relay nuclei of basal ganglia output. Activation maps were coregistered onto a 3-D brain atlas. Based on calbindin immunohistochemistry data, the atlas locates the associative, the sensorimotor and the limbic territories of the striatum, the globus pallidus and the subthalamic nucleus (Karachi *et al.*, 2002), allowing a precise localization of basal ganglia activation.

To differentiate activation in the motor, premotor and associative territories of basal ganglia circuits, we varied both the frequency (from 0.5 to 3 Hz) and the complexity of finger movements (a repetitive finger movement, a simple sequence of finger movement, and a complex sequence of 10 moves). Based on previous reports describing the role of the frontal areas in motor control, it was expected that (i) activation in the sensorimotor circuit of the basal ganglia would correlate with movement frequency only; (ii) the premotor circuit would be modulated by movement complexity and frequency; and (iii) the associative circuit would be activated during the more complex sequences of finger movement only.

Materials and Methods

Subjects

Twelve right-handed healthy volunteers were studied (nine women; mean age = 22.9 ± 3.9 years, age range = 18–33 years). Volunteers were college students. All subjects gave informed consent. Handedness was confirmed by a test of laterality (Edinburgh Handedness Inventory). All subjects were strongly right handed. None of the subjects was a musician. Two subjects used to play the piano but stopped at least 7 years before the time of the study. The Local Ethics Committee approved the study.

Imaging

The MR protocol was carried out using at 3 Tesla whole-body system (Siemens, Erlangen, Germany) using blood oxygen level-dependent (BOLD) fMRI. The head of the subject was immobilized using foam cushions and tape, with their ears plugged. The protocol included: (i) one sagittal T_1-weighted image to localize functional and anatomical axial slices; (ii) 28 axial gradient echo echo-planar images (EPI) (2.5 mm no gap, T_R = 3 s, T_E = 40 ms, bandwidth = 1562 Hz/pixel, $\alpha = 90°$, FOV = 192 × 192 mm^2, matrix size = 128 × 128, in-plane resolution = 1.5 × 1.5 mm, partial Fourier imaging 6/8). For each series, 144 EPI volumes were acquired over 7 min 12 s. The first four volumes of each run were discarded to reach signal equilibrium; and (iii) 144 sagittal 3-D MP-RAGE images (1 mm thick, FOV = 256 × 256 mm^2, matrix size = 256 × 256) for anatomical localization. The whole protocol lasted ~90 min.

Tasks

Complexity Study

The tasks consisted of three conditions of sequential key press on a keyboard using fingers 2–5 of the right hand: (i) a simple repetitive flexion of the index finger (Simple task); (ii) a scale finger tapping (digits 2–3–4–5 = Scale task); and (iii) a complex sequence of 10 moves (2–4–3–5–4–2–5–3–4–5 = Complex task). Before scanning, all subjects practiced the Complex task until they could perform it from memory 10 times in a row without any error. Thus, tasks varied several motor components of increasing complexity: no sequence (Simple) versus sequential movements (Scale and Complex), short (Scale) versus long sequence (Complex), no higher-order motor components (Simple and Scale tasks) versus higher-order motor components such as working memory (Complex task). For each series, subjects alternated 10 epochs of 21 s of rest and motor conditions (seven images over 21 s during the motor condition followed by seven images over 21 s during the rest condition). Task switching was indicated using audio cues at the beginning and end of each epoch (i.e. 'action' and 'rest'). The order of the tasks was pseudo-randomly determined across subjects. Movements were audio-paced with computer-generated sounds at a fixed frequency of 1 Hz and transmitted to the subjects using headphones. During the rest condition, subjects were told to remain in a resting awake state while listening to the beat of the metronome.

Frequency Study

Subjects performed the Scale task using the right hand (digits 2–5 sequentially). Finger movement frequency was driven by the external pacing at five different frequencies (0.5, 0.67, 1, 2 and 3 Hz). The control condition was rest. Subjects performed five series alternating 10 epochs of 21 s of motor and rest conditions. Each series comprised two occurrences of each frequency, and the order of presentation of the different frequencies was pseudo-randomly arranged within and across series to minimize potential time and order effects. Each frequency was presented 10 times in total. During the scan, the subjects laid in the dark with eyes closed. The beat of the metronome was stopped during the rest condition. Task switching was indicated at the beginning and the end by the metronome.

Software was written using Matlab (The Mathworks, Inc.). The keyboard was customized for an MRI environment (Electrical Geodesics, Inc. Eugene, OR), allowing for recording of responses and timing. Subjects were required to keep their fingers on the keys at all times to minimize amplitude variation. The amount of force required to press the keys was minimal. All tasks were audio driven and there was no visual instruction.

FMRI Data Analysis

Data analysis was first performed with SPM99 (Wellcome Department of Cognitive Neuroscience, London). For each subject, anatomical images were transformed stereotactically to Talairach coordinates with a voxel size of 2 × 2 × 2 mm. The functional scans, corrected for subject motion (Friston *et al.*, 1995), were then normalized using the same transformation and smoothed with a Gaussian spatial filter to a final smoothness of 10 mm. Data were analyzed across subjects (group analysis using random effect). Data from each voxel were modeled using the general linear model with separate hemodynamic response functions and their time derivatives modeling each period of the tasks. Overall signal differences between runs were also modeled. A 240 s temporal cut-off was applied to filter subject-specific low frequency drift of the signal. To test hypotheses about regionally specific condition effects, the estimates were compared using linear contrast associated with the motor and rest conditions. The resulting set of voxel values for each contrast constituted an SPM$\{t\}$ map, which was transformed to the unit normal distribution to give an SPM$\{Z\}$ map. Zmaps were first thresholded at $P < 0.001$. In these maps, activated clusters were considered significant at $P < 0.05$ corrected for multiple comparisons inside the volume of the whole brain (for cortical activation), inside the volume of the striatum (for caudate nucleus and putamen) or inside the thalamus (small volume correction) unless stated otherwise. In this case, the small volume correction is valid because the statistical analysis is guided by a very strong anatomical hypothesis, with well-defined and invariant anatomical landmarks across subjects (Worsley *et al.*, 1996). The volume of basal ganglia nuclei and the thalamus were created for each control using semiautomatic segmentation (MRIcro). Since the globus pallidus and the subthalamic nucleus had a low signal on EPI images, these structures were often not included in the default mask provided by SPM99, which categorizes voxels as part of the brain or the background noise. This mask

was altered to include all basal ganglia structures, the thalamus, the adjacent white matter and the upper part of the mesencephalon. Calculations were then performed inside the volume of the mask only.

Subtraction Analysis

To identify areas activated during each task, all motor conditions were first compared with the rest conditions. To identify areas activated with complex movement sequencing, the Complex task was compared with the Scale and Simple tasks. To identify areas activated with simple movement sequencing, the Scale task was compared with the Simple task.

Analysis of Signal Variations Profiles

To identify regions associated with different activation patterns between the Simple, Scale and Complex tasks, and with a correlation between movement frequency and signal increase, we performed post-hoc statistical analyses on individual percentages of signal increase in the areas activated in the subtraction analysis in each of the three territories. Signal-to-time curves were calculated for voxels located inside regions activated in the group study to determine pattern of signal changes in the different cortico-basal ganglia circuits. These curves were obtained by averaging the signal of individual data points (corresponding to the activated voxel of peak *Z* score in each region and in each subject) across trials of the same types and then averaging across subjects, leading to a mean time-course of fMRI signal for each task. All subsequent coordinates are *x*, *y* and *z* Talairach coordinates, in mm. These regions included three cortical [SMC, –36.2 ± 3.0, –22.3 ± 4.6, 57.0 ± 6.1; premotor (SMA), –2.3 ± 1.7, –3.5 ± 3.9, 55.0 ± 5.5; and dorsolateral prefrontal cortex (DLPFC), –34.4 ± 12.0, –33.1 ± 9.6, 32.7 ± 7.1], three striatal regions (posterior putamen caudal to the anterior commissure, –24.6 ± 3.6, –0.6 ± 5.9, 3.4 ± 9.0; anterior putamen rostral to the anterior commissure, –22.5 ± 2.8, 8.2 ± 6.1, 2.4 ± 3.0; and caudate nucleus, –13.7 ± 6.3, 9.7 ± 11.5, 9.4 ± 9.7), two territories of the globus pallidus (anterodorsal, –18.4 ± 1.3, 1.6 ± 2.4, 2.0 ± 5.4, which corresponds to the associative territory, and posterior, –21.3 ± 2.0, –4.7 ± 3.5, 2.8 ± 2.8, which corresponds to the sensorimotor territory) (Middleton and Strick, 2000), the thalamus [ventrolateral/ventral anterior nuclei (VA/VL), –10.8 ± 3.7, –8.8 ± 5.7, 9.0 ± 5.1 and the ventral intermediate (Vim), –14.9 ± 3.0, –16.9 ± 3.6, 8.7 ± 4.6] and the STN (which was too small for separate analysis of different territories, 11.6 ± 4.1, –10.0 ± 2.8, –4.9 ± 4.1). Analysis was conducted using statistical software (SPSS Inc., version 11.5, Chicago, IL). In the complexity study, statistical comparisons were performed using non-parametric procedures because of repeated violations of the assumption of distribution normality. A Friedman test for multiple related samples (allowing comparing multiple series in multiple subjects) was first conducted for all regions and all tasks to determine whether the signal increase was equally distributed or not. The dependent variable was the percent signal increase between each of the three tasks and the regions of interest in the left hemisphere. The Friedman test between all regions was significant ($P < 0.001$). Second, the signal was averaged for each task across all regions, and a Friedman test was conducted between tasks. This comparison showed a significant difference between tasks ($P < 0.001$). Third, Friedman tests were conducted between tasks in each region and showed significant differences in signal increase between tasks in all regions except the posterior putamen. Comparisons using a Wilcoxon test were conducted between tasks in each region to determine whether the percent signal increase differed between the three tasks. Results of these latter comparisons are presented in the Results section. All values are expressed as mean ± SD. The significance level was set at $P < 0.05$. Correlations between signal increase and movement frequency were performed using Pearson's correlation.

Anatomical Localization of Basal Ganglia and Thalamic Activation

Activation in the basal ganglia and thalamus was located by coregistering MR images with a multimodal and deformable atlas based on histological and MR data (Yelnik *et al.*, 2003). Atlas contours were drawn from a human brain obtained at autopsy from body donation and T_1- and T_2-weighted images were obtained before extraction. The brain was selected using the following criteria: post-mortem delay <48 h, absence of neurologic or psychiatric diseases, absence of vascular or neurosurgical pathology, and absence of intensive care before death. After MR scans, the left hemisphere was fixed in formalin solution for 24 h, cut into 1.5-cm-thick frontal blocks that were fixed for 8 days and cut into 70-μm-thick frontal sections on a freezing Microtome. Photographs of the frozen blocks were taken every ten sections. The 800 sections obtained were collected serially. One series of sections was Nissl-stained. Another adjacent series was immunostained for calbindin (Karachi *et al.*, 2002). Contours of cerebral regions of the basal ganglia (striatum, globus pallidus, substantia nigra and subthalamic nucleus), their functional subterritories (sensorimotor, associative and limbic) and some related structures (red nucleus) were delimited on the basis of Nissl-staining and immunohistochemistry of calbindin. Parcelation of the thalamus was based on cytoarchitectonic criteria (Percheron *et al.*, 1996) and calbindin immunohistochemistery (Morel *et al.*, 1997). Contours were optimized by confronting all coregistered atlas data. The photographs of the frozen sections were aligned by using fiducial markers to obtain a geometrically consistent 3-D 'cryo-block' which was registered with the T_1-MR and T_2-MR images. Each histological section was registered onto the corresponding cryo-block, compensating for histological processing distortions, thus providing 3-D 'histo-blocks'. All registrations were performed by applying the same automatic intensity-based method to a region of interest centered on the basal ganglia. Surfaces were generated from the serially optimized contours, yielding a true 3-D atlas of the basal ganglia which could be sliced in any orientation.

Automatic coregistration between atlas and subjects' T_1-weighted MR images was performed on the basis of regions of interest automatically defined around the basal ganglia using local affine transformations. Surfaces of atlas structures were deformed into the geometry of the different subjects following these transformations. Reliability of coregistration was verified by the observation that structures visible in T_1-weighted MR sequences (caudate nucleus, putamen, cerebral peduncle, mamillo-thalamic tract and anterior column of the fornix) were reliably delineated by a histology-based atlas.

Results

Behavioral Data

Movement Complexity

There was no difference in the observed movement frequencies between tasks (Simple task = 0.97 ± 0.01 Hz, Scale task = 0.97 ± 0.01 Hz, Complex task = 0.98 ± 0.01 Hz). The number of errors (incorrect taps) was low in all tasks, and the difference was not significant although there were more errors in the Complex than in the two other tasks [mean number of errors ± SD: Simple task = 0.3 ± 0.9, Scale task = 0.5 ± 1.2, Complex task = 3.1 ± 3.8, analysis of variance (ANOVA) for repeated measurements, $P = 0.12$].

Movement Frequency

Subjects performed the tasks at the expected frequency ± 1.3% for all five frequencies. The number of errors (incorrect taps) was low in all tasks and did not differ between frequencies, although there were a few more errors at 3 Hz (0.5 Hz = 1.58 ± 1.73, 0.67 Hz = 1.25 ± 1.29, 1 Hz = 0.92 ± 2.02, 2 Hz = 1.50 ± 1.98, 3 Hz = 1.92 ± 2.47, ANOVA for repeated measurements, $P = 0.07$).

fMRI Data

Areas Modulated by the Frequency but Not the Complexity of Movement Sequence

This activation pattern was observed in the SMC, the putamen posterior to the anterior commissure and the adjacent posterior (sensorimotor) globus pallidus (Table 1). For the complexity study, the SPM analysis showed that the contralateral SMC was

Table 1
Talairach coordinates of cluster maxima during each contrast

Activated areas	Henosphere	BA	Simple–rest				Scale–rest				Complex–rest				Complex–Simple				Complex–Scale				Scale–Simple			
			x	*y*	*z*	*Z* score (*n*)	*x*	*y*	*z*	*Z* score (*n*)	*x*	*y*	*z*	*Z* score (*n*)	*x*	*y*	*z*	*Z* score	*x*	*y*	*z*	*Z* score	*x*	*y*	*z*	*Z* score
Cortex																										
SM1	L	4	−40	−14	50	6.34	−44	−24	56	8.13	−36	−22	56	6.59	−36	−22	58	8.19					−34	−28	60	9.57
SMA	L	6	*−2*	*−4*	*56*	*4.81*	−2	−2	56	6.45	−6	−4	54	5.72	−2	−4	50	6.76					*−4*	*−6*	*52*	*5.20*
preSMA											−2	0	52	6.64	−4	2	48	5.47	0	6	52	4.85				
PM	L	6									−26	−8	52	6.91	−30	−10	58	10.45	−14	0	52	8.57	−24	−10	62	4.50
	R										28	−2	40	6.13	34	0	62	6.34	38	−4	46	7.32				
ACC	L						−6	2	46	5.90	−10	6	42	4.26	−8	8	38	6.37								
	R										16	8	38	4.42	14	6	38	6.6								
PF	L	44					*−46*	*6*	*6*	*5.74*	*−60*	*10*	*24*	*6.42*	−56	8	32	5.16								
	R										*50*	*16*	*12*	*4.39*	54	−10	30	4.87								
	R	9/46									*34*	*30*	*16*	*4.31*	32	48	18	9.97	*38*	*28*	*16*	*5.64*				
SII	L		*−42*	*−26*	*22*	*6.52*	*−48*	*−20*	*28*	*5.52*	−52	−20	32	5.59	−52	−26	38	5.75								
	R														56	−20	36	5.24								
Parietal	L	40									−46	−26	52	8.15	−44	−30	50	12.26	−44	−36	48	6.99				
	R														46	−40	58	6.7	34	−44	48	6.97				
	L	7									−20	−66	62	4.38	−14	−62	68	9.39	−28	−60	58	7.25	−36	−46	66	5.01
	R										30	−64	52	8.82	24	−64	56	8.68	26	−66	56	9.97				
IPS	L										−32	−40	46	8.03	−32	−38	48	11.73	−26	−54	48	7.10				
	R										40	−50	44	6.97	34	−42	48	6.37								
Precuneus	L										−10	−66	56	6.20	−8	−64	54	6.82	−8	−64	54	9.03				
Insula	L										−24	−20	14	7.18	−28	20	8	6.58								
Basal ganglia																										
Putamen	L		−34	0	0	9.93 (9)	−22	16	4	6.97 (10)	−24	4	0	4.75 (10)	−24	14	12	5.72					*−30*	*8*	*4*	*4.35*
	R		28	4	14	7.62	22	18	6	5.07	26	10	16	6.14	18	10	2	5.22	*26*	*12*	*14*	*4.10*	*14*	*12*	*2*	*6.13*
CN	L					(0)	−18	14	4	6.00 (5)	−14	14	4	6.39 (8)	8	16	10	6.66	−18	−24	22	5.70				
	R										20	12	20	8.47	−12	−2	16	7.34					14	12	2	6.13
GP	L		−18	−2	12	7.33 (8)	−20	2	0	5.92 (7)	−18	−10	2	5.72 (9)	−14	4	4	5.8								
	R		12	2	0	5.73					20	−6	0	4.66	16	6	4	5.89								
STN	L					(0)	−14	−16	−2	5.15 (1)	−12	−12	−4	4.36 (7)	−12	−12	−4	5.08								
	R										10	−12	−6	4.76	14	−12	−4	4.53	10	−12	−6	4.75				
Thalamus	L		−14	−16	8	5.71 (4)	−14	−16	2	4.88 (9)	−14	−12	10	6.72 (11)	−10	−10	12	6.48	−14	−14	12	4.39				
	R														10	−2	10	5.18	8	−16	18	4.49				

Abbreviations: ACC = anterior cingulate cortex, BA = Brodmann area, CN = caudate nucleus, GP = globus pallidus, IPS = intraparietal sulcus, L = left, PF = prefrontal cortex, PM = premotor cortex, R = right, SM1 = sensorimotor cortex, SMA = supplementary motor area, STN = subthalamic nucleus. Activated clusters were significant at $P < 0.05$ corrected for multiple comparisons (figures in italics show the activation trends at $P < 0.001$, not corrected). The figures in brackets indicate the number of subjects who presented activation in the basal ganglia and thalamus in the hemisphere contralateral to the moving hand using the same statistical threshold as for the group study.

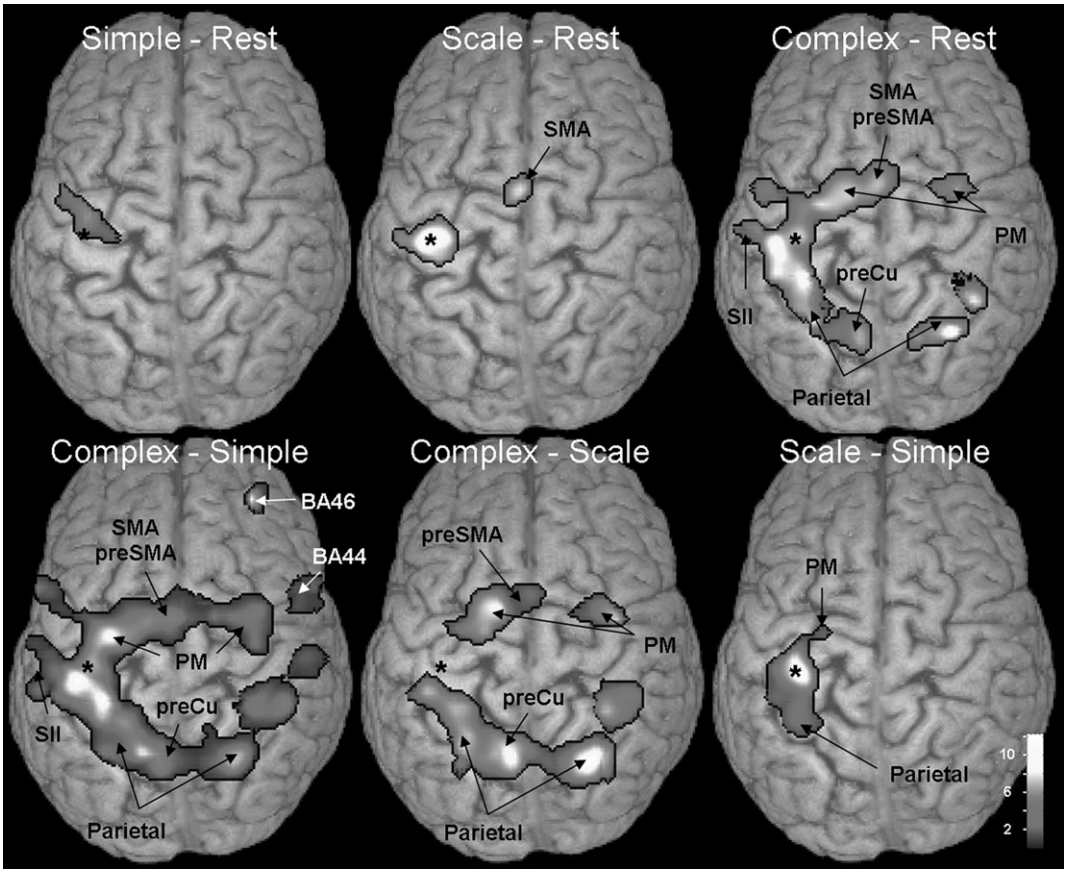

Figure 1. Cortical activation observed during the complexity tasks (random effect analysis, activation clusters are shown at $P > 0.05$ corrected for multiple comparison) projected on a three dimensional surface rendering of a brain template. Color scale indicates *Z*-score range. BA = Brodmann area, PM = lateral premotor cortex (BA6), preCu = precuneus, SII = secondary sensory area, SMA = supplementary motor area. The asterisk indicates the central sulcus.

more activated in the Complex and Scale tasks than in the Simple task, but that the signal intensity did not differ between the Complex and Scale tasks (Fig. 1). There was no significant difference between all three tasks in the posterior putamen and the globus pallidus (Figs 2–4). In the SMC, the percentage signal increase was significantly smaller in the Simple task than in the two other tasks ($P < 0.001$) whereas there was no difference between the Scale and Complex tasks (Fig. 5). In the posterior part of the globus pallidus, the same pattern was observed except that the difference in signal increase between the Simple and Scale tasks did not reach significance ($P < 0.11$). In the posterior putamen, although signal increase was lower in the Simple task (0.55 ± 0.58%) than in the two other tasks (Scale: 0.71 ± 0.88% and Complex: 0.68 ± 0.27%), this difference did not reach significance.

Signal increase and movement frequency were significantly correlated in the contralateral SMC ($r^2 = 0.929$, $P = 0.008$) and the posterior putamen ($r^2 = 0.988$, $P = 0.0005$) (Fig. 6). Overall, the correlation was best fitted with a linear function. In the SMC, there was an increase in signal change of ~0.8% per Hz. In the putamen, the rate dependence was much lower than in the SMC (~0.23% per Hz).

Areas Modulated by the Complexity and the Frequency of Movement

This activation pattern was observed in the posterior premotor cortex, the SMA (Fig. 1), the putamen rostral to the anterior commissure and the Vim nucleus of the thalamus (Figs 2–4) (Table 1). The SPM analysis showed that the left SMA, the lateral premotor (PM = BA6) and the superior parietal areas (BA7) were activated to a greater degree (i) in the Complex task than in the Simple and the Scale tasks; and (ii) in the Scale task than in the Simple task (Fig. 1), although there were only activation trends in the SMA for the latter comparison ($P < 0.001$ not corrected). Activation in bilateral anterior putamen and the Vim nucleus of the thalamus was observed during the Scale and Complex tasks (Figs 2–4). Direct comparison between tasks showed that (i) the bilateral anterior putamen was more activated in the Complex than in the Simple task (Figs 2–4); (ii) the anterior putamen in the right hemisphere was more activated in the Complex than in the Scale task (Fig. 2); and (iii) the bilateral anterior putamen were more activated in the Scale than in the Simple task at a more liberal threshold (height threshold at $P < 0.01$, clusters significant at $P < 0.05$ corrected). The statistical analysis on percentage signal increase showed that signal in the left SMA, the anterior putamen and the Vim thalamus increased significantly between the Simple and Scale tasks, and between the Scale and Complex tasks (all *P*-values < 0.05, Fig. 5). A significant linear correlation between signal increase and movement frequencies was found in the contralateral SMA ($r^2 = 0.981$, $P = 0.001$), the anterior putamen ($r^2 = 0.81$, $P = 0.0038$) and the Vim nucleus of the thalamus ($r^2 = 0.949$, $P = 0.005$) (Fig. 6).

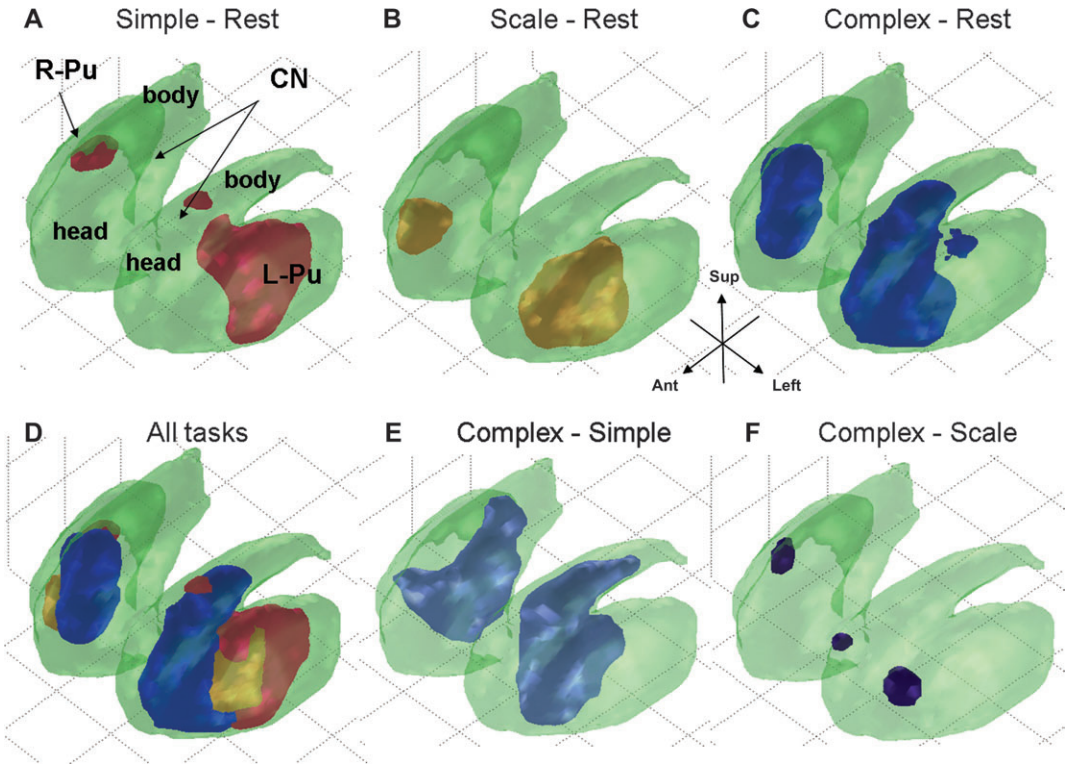

Figure 2. Oblique three dimensional views of striatal activation during the Simple (*A*), Scale (*B*), and Complex tasks (*C*) compared with rest, all three tasks (*D*), and the Complex versus Simple (*E*) and Complex versus Scale (*F*) comparisons (random effect group study, cluster activated at $P < 0.05$, corrected for the volume of the striatum). The striatum is represented in an oblique view as if viewed from anterior and left. Ant = anterior, CN = caudate nucleus, L-Pu = left putamen, R-PU = right putamen, Sup = superior.

Areas Activated during the Complex Task Only and Not Modulated by Movement Frequency

This pattern was observed in rostral frontal and parietal associative areas, the caudate nucleus, the subthalamic nucleus and the VA/VL thalamus (Table 1). The SPM analysis showed that the left preSMA and precuneus, bilateral PM (BA6) and posterior parietal areas (BA40, intraparietal sulcus) were significantly more activated during the Complex task than during the two other tasks (Fig. 1). The right DLPFC (BA46) was more activated during the Complex than the Simple task, and there were also activation trends in the same region during the Complex versus Scale comparison ($P < 0.001$ not corrected). Except for a small cluster in the left caudate nucleus activated during the Scale task compared with rest, activation in the caudate nuclei, the anterodorsal (associative) parts of the globus pallidus and the left VA/VL nuclei of the thalamus were only observed when the Complex task was compared with rest (Fig. 2). STN activation was observed in the left hemisphere during the Scale task and in both hemispheres during the Complex task (Figs 3 and 4). Left STN activation extended toward the adjacent SN in the Complex task (Fig. 4). Although no activation was detected in the STN during the Simple task, there was a clear extension of pallidal activation toward the superior and anterior part of the STN (Figs 3 and 4). Direct comparison between tasks showed that (i) the caudate nuclei, the anterodorsal globus pallidus, the STN and the anterior thalamus were more activated bilaterally in the Complex than in the Simple task (Figs 2–4); (ii) the left caudate nucleus (Fig. 2), the right STN and bilateral VA/VL nuclei of the thalamus were more activated in the Complex than in the Scale task; and (iii) only a small cluster in the right caudate nucleus was more activated in the Scale than in the Simple task.

The statistical analysis on percentage signal increase confirmed that signal increase was significantly larger during the Complex task than in the two other tasks, and did not differ between the Simple and the Scale tasks in the following regions: the right prefrontal cortex, the caudate nucleus, the anterodorsal part of the globus pallidus, the STN and the VA/VL thalamus in the left hemisphere (Fig. 5). In the frequency study, there was no significant signal increase in the caudate nucleus, although a small but not significant signal increase was observed in the 2 and 3 Hz conditions. In the left STN, signal increase did not differ at low frequencies (between 0.5 and 1 Hz) but increased at the highest frequencies (2 and 3 Hz), and the correlation between signal increase and frequency was best fitted with a second-order polynomial function ($r^2 = 0.97$, Fig. 6).

STN Activation

Because activation in the STN area sometimes merged with adjacent activated areas, such as the globus pallidus or the thalamus, we further investigated the STN origin of activation in this area. To determine whether activation in the STN area was the result of a blurring effect from adjacent activation due to the Gaussian spatial filter or was truly STN activation, basal ganglia analysis was repeated with different filter sizes [full-width half-maximum (FWHM) ranging from 4 to 10 mm]. Reducing the filter size resulted in a reduction of the size and *P*-values of activated clusters. Talairach coordinates of the activation peak remained consistent (Fig. 7). *Z* scores of activation peaks were similar between 10 and 6 mm, but decreased below 5 mm. The STN activation was easily differentiated from the thalamic activation (above) and from the SN (below), although activation merged for filter sizes greater than 6–7 mm. Thus, smoothing

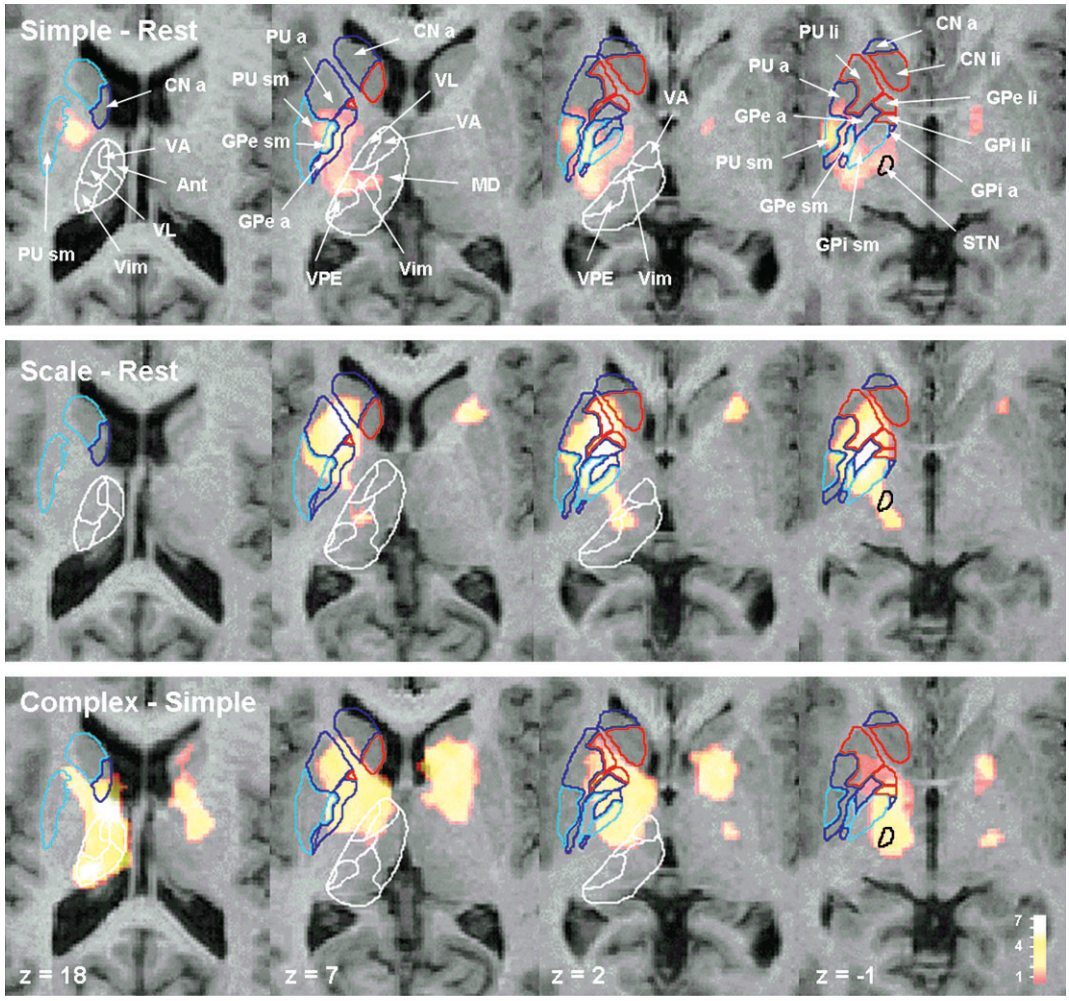

Figure 3. Axial views of activation maps obtained during the Simple versus rest (upper row), Scale versus rest (middle row) and Complex versus Simple (lower row) comparisons superimposed the anatomical images of a brain template (random effect group study, cluster activated at $P < 0.05$ corrected). The atlas is superimposed on the activation maps. The sensorimotor (light blue), associative (dark blue) and limbic (red) territories are delineated in the striatum and globus pallidus. Thalamic nuclei (white), the STN (black), SN (purple) and RN (yellow) are also outlined. Dorsal is left, ventral is right. The *z*-coordinate of each image is indicated in the lower row (in mm). Color scale indicates *Z*-score range. Ant = anterior nucleus, a = associative, CN = caudate nucleus, GPe = external part of the globus pallidus, GPi = internal part of the globus pallidus, li = limbic, post = posterior, MD = mediodorsal nucleus, PU = putamen, sm = sensorimotor, RN = red nucleus, SN = substantia nigra, STN = subthalamic nucleus, VA = ventral anterior nucleus, VPE = ventral posterior external nucleus, Vim = ventral intermediate nucleus, VL = ventral lateral nucleus.

data up to 10 mm FWHM resulted in increased significance and size of STN activation, and blurring was still acceptable.

Discussion

Optimized Detection of Activation in Small Basal Ganglia Structures

Activation was detected in all basal ganglia structures. The study design was chosen to maximize signal detection in the basal ganglia. Higher field strength allowed increased spatial resolution with a voxel size of 5.6 mm^3, as compared with 30–60 mm^3 in most fMRI studies performed at 1.5 T. At such a low spatial resolution only a few voxels included the STN, and partial voluming was high. A simple block-design protocol was chosen, as functional contrast of blocked-design fMRI can be 35% larger than that of event-related fMRI (Bandettini and Cox, 2000). Subjects performed long series of finger movements of optimal duration. This task design was chosen over a factorial design mixing of the rate and complexity factors because collecting more data samples helps detecting voxels with low contrast-to-noise ratio (Saad *et al.*, 2003). The use of a specific mask for basal ganglia analysis also improved activation detection in the basal ganglia (see Materials and Methods).

It was also critical to ascertain the origin of STN activation. First, the coordinates of the peak *Z* score corresponded to those of the STN in stereotactic atlases (Talairach and Tournoux, 1988). Second, activation was located within the small area of low signal intensity on T_2*-weighted EPI images, located laterally and superiorly to the low signal of the SN (Fig. 7), an area recently described as corresponding to the STN (Dormont *et al.*, 2004). Third, comparison of different spatial filter size confirmed that STN activation did not result from blurring of activity from neighboring structures. Spatial filtering of data is necessary for group analysis to compensate for the anatomic and functional variability between individuals (Poline and Mazoyer, 1994; Kruggel *et al.*, 1999). The filter size should be large enough to mix functionally homologous regions in individuals but small enough not to blur distinct regions. We chose a 10 mm filter size as this size was necessary to detect cortical activation and was commonly used in random effect group studies (Poline and

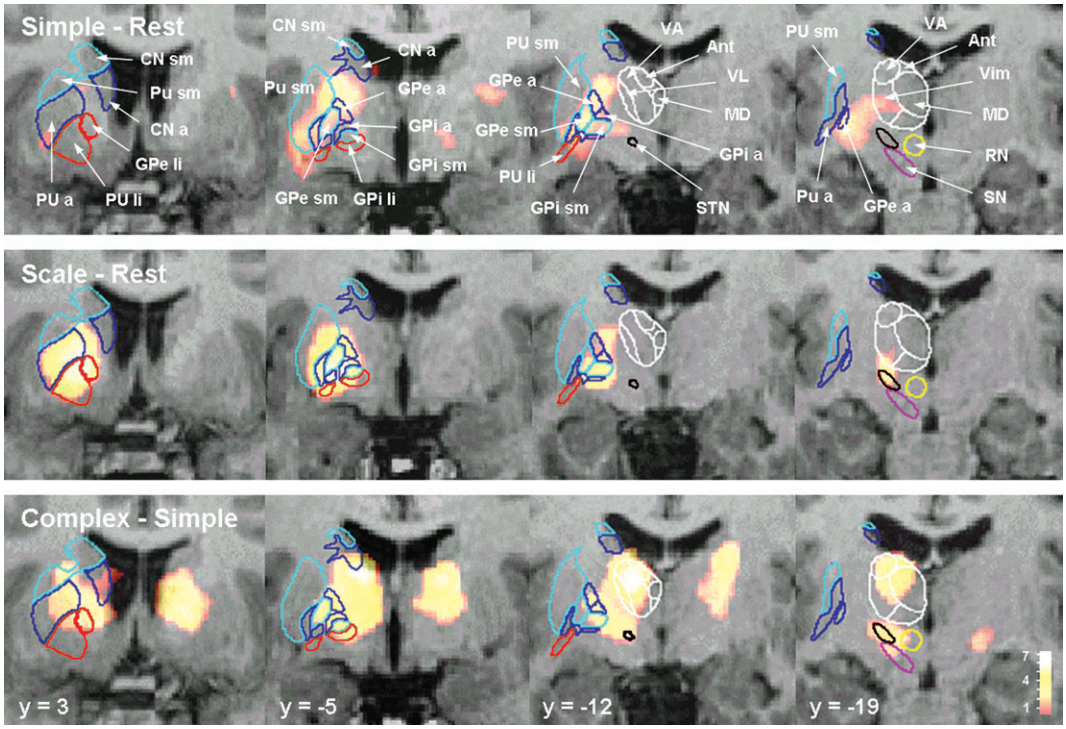

Figure 4. Coronal views of activation maps obtained during the Simple versus rest (upper row), Scale versus rest (middle row) and Complex versus Simple (lower row) comparisons superimposed on the anatomical images of a brain template (random effect group study, cluster activated at $P < 0.05$ corrected). Rostral is left, caudal is right. Color coding and abbreviations are as is as defined in Figure 3. The *y*-coordinate of each image is indicated in the lower row.

Mazoyer, 1994). However, the present results confirmed that smaller filter size may be optimal for subcortical structures as individual foci merged at filter sizes larger than 6–7 mm (White *et al.*, 2001). By contrast, activation peaks in the STN did not vary with filter size and all peaks were within the area of the STN. Lastly, the atlas allowed precise localization of activation in basal ganglia structures and thalamic nuclei. This proved particularly useful in distinguishing activation in the STN from the neighboring thalamic and SN activation.

Activation Patterns in Basal Ganglia Circuits

Schematically, three main patterns of activation were observed in cortico-basal ganglia structures. Signal in the posterior putamen and the posterior globus pallidus was not modulated by the complexity of movement sequence, suggesting that these areas do not control this parameter, in agreement with previous studies in monkeys (Mushiake *et al.*, 1991) and humans (Shibasaki *et al.*, 1993; Sadato *et al.*, 1996a; Boecker *et al.*, 1998; Catalan *et al.*, 1998; Harrington *et al.*, 2000). A similar pattern was observed in the SMC, in which signal did not differ between the Scale and Complex tasks. Data in the SMC are in line with the previous imaging studies in humans, which showed a larger activation in this region when movements involved more fingers (Colebatch *et al.*, 1991; Catalan *et al.*, 1998; Hlustik *et al.*, 2001) but no difference between complex and simple sequences (Sadato *et al.*, 1996a; Boecker *et al.*, 1998; Catalan *et al.*, 1998). In the posterior putamen, there was a clear but mild rate-dependence of signal increase. In the posterior putamen, this rate-dependence cannot be explained by a learning effect or by a time effect, as the order of each frequency was randomized across series. The amplitude of movement was also kept constant as the fingers always rested on the keys. However, we cannot rule out that changes in movement frequency may also be associated with changes in movement acceleration or velocity, which increase with movement frequency. The rate dependence of the putamen was much lower than in the SMC. Although numerous studies have reported that magnitude of activation correlated with movement frequency in the SMC and premotor areas (Rao *et al.*, 1996; Jenkins *et al.*, 1997; Sadato *et al.*, 1997; Wexler *et al.*, 1997; Kawashima *et al.*, 1999), the striatum has received considerably less attention. One report studied the frequency dependence of striatal activation (Jenkins *et al.*, 1997). In this study, the frequency of movement did not correlate with the magnitude of rCBF changes in the putamen (Jenkins *et al.*, 1997). The discrepancy with the present results may be due to differences in the motor tasks, the sensitivity of the techniques or the frequency range used, as our results were obtained with a faster frequency range (Jenkins *et al.*, 1997). In this study, joystick movement in freely selected direction was associated with activation in the striatum more rostral than in the present study (Jenkins *et al.*, 1997). The mild dependence of signal intensity on movement frequency in the putamen as compared with the SMC is also in line with the observation that the striatum is not a key structure in controlling basic movement parameters (Mink, 1996).

In premotor areas, the anterior putamen and the Vim nucleus of the thalamus, activation increased regularly from the Simple to the Complex finger tapping task and was modulated by the frequency of finger tapping. Sequential finger movements were processed in more rostral regions of the striatum than during simple repetitive movement. Since subjects used only one finger during the Simple task and four fingers during the Scale and Complex tasks, it can be argued that the difference in the location of activation between the Simple and Scale tasks may

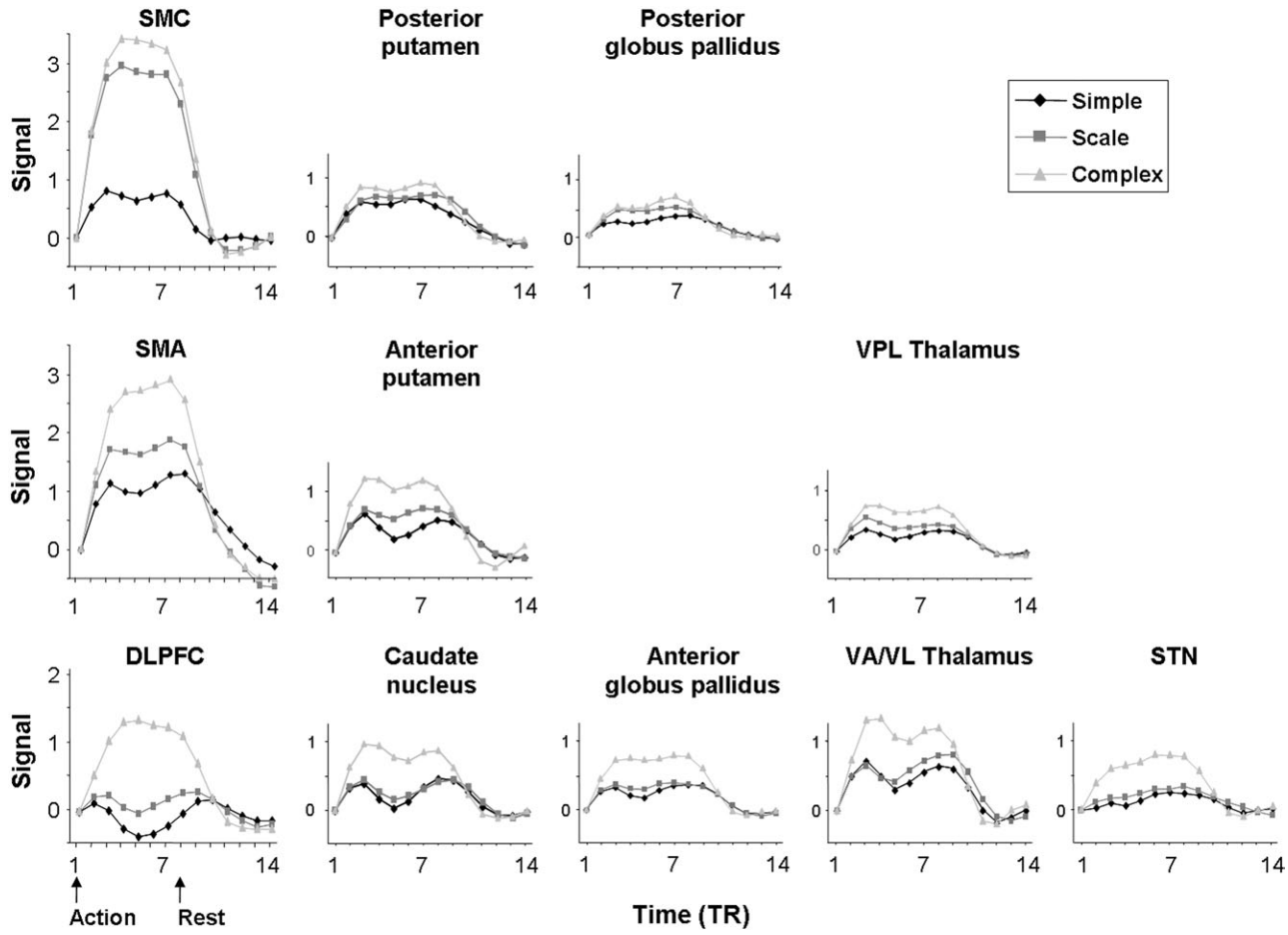

Figure 5. BOLD responses during the Simple, Scale and Complex tasks. Upper row: regions not modulated by movement complexity; middle row: regions with progressive signal increase from the Simple task to the Complex task; lower row: regions with a larger signal increase in the Complex than in the two other tasks. Signal versus time curves were obtained by averaging the signal of individual data points across trials of the same types and then by averaging across subjects (for mean Talairach coordinates, see Materials and Methods).

be due to a difference in somatotopy. However, previous studies also reported activation located in the posterior putamen during performance of simple, non-sequential finger movements involving all digits, a finding which argues against this hypothesis (e.g. flexion–extension of the digits) (Lehéricy *et al.*, 1998; Maillard *et al.*, 2000; Gerardin *et al.*, 2003). In monkeys, few studies have examined the role of the striatum in movement sequences (Alexander and Crutcher, 1990; Kimura, 1990, 1992; Kermadi *et al.*, 1993; Miyachi *et al.*, 1997). Activity related to the onset and to each movement of the sequence was reported in monkeys performing a sequence of three flexion–extensions of the arm (Kimura, 1990). These studies did not mention whether activity during sequential movements was located rostral to non sequential movements. Other functions attributed to premotor areas, such as set-related activity, were located rostral to movement related activity in the striatum (Alexander and Crutcher, 1990; Kimura, 1990; Schultz and Romo, 1992). In the globus pallidus, electrophysiological studies in monkeys have reported neurons that were preferentially active during sequential movements (Brotchie *et al.*, 1991; Mushiake and Strick, 1995), and activity in some of these neurons depended on the specific sequence that was to be performed (Mushiake and Strick, 1995). These neurons were located in the dorsomedial part of the globus pallidus. In humans, increased activation which correlated with the length of sequences of finger movements has been observed in the globus pallidus and the thalamus using positron emission tomography (Boecker *et al.*, 1998). At the cortical level, previous studies have shown that premotor and parietal areas were recruited during performance of a sequential movement (Roland *et al.*, 1982; Colebatch *et al.*, 1991; Rao *et al.*, 1993, 1996; Shibasaki *et al.*, 1993; Sadato *et al.*, 1996a; Jueptner *et al.*, 1997b; Boecker *et al.*, 1998; Catalan *et al.*, 1998; Gordon *et al.*, 1998; Harrington *et al.*, 2000). Posterior premotor areas, including the SMA, also correlated with movement frequency (Jenkins *et al.*, 1997), suggesting an executive role in running sequences, whereas activation in the preSMA, the ipsilateral premotor cortex and the precuneus was positively correlated with the length of sequences of finger movement (Boecker *et al.*, 1998; Catalan *et al.*, 1998; Harrington *et al.*, 2000; Haslinger *et al.*, 2002), suggesting a more specific role in the control of sequence complexity. These results are in line with the present findings, showing that the preSMA, the ipsilateral premotor cortex and the precuneus were more activated during the Complex task than during the two other tasks.

Activation in prefrontal areas, the caudate nucleus, the anterodorsal globus pallidus, the subthalamic nucleus and the ventral anterior thalamus showed a similar pattern of signal increase, characterized by low or no signal increase during the Simple

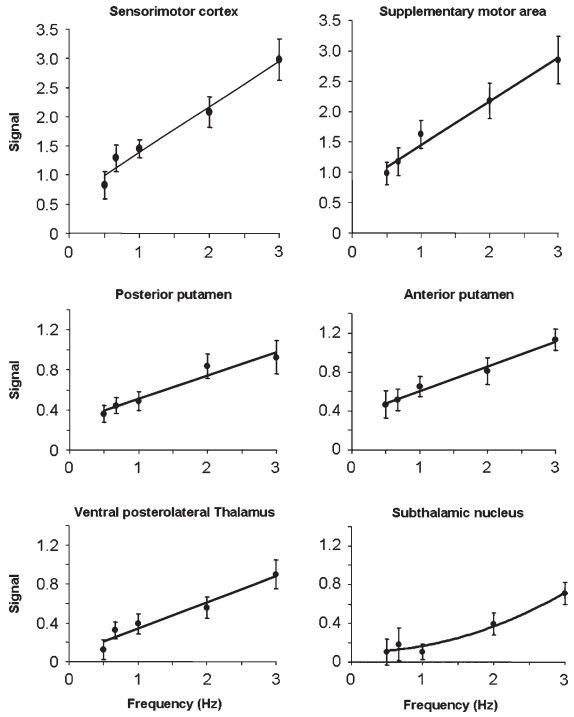

Figure 6. Graphs showing the mean ± SEM signal increase across all subjects in the left hemisphere during the Scale task at the five different frequencies. Signal versus time curves were obtained by averaging the signal of individual data points across trials of the same types and then by averaging across subjects. There was a correlation between signal increase and frequency in all regions. In the STN, signal increase did not vary between 0.5 and 1 Hz, but increased at 2 Hz and 3 Hz. Time is in T_R ($T_R = 3$ s).

and Scale tasks at low frequency and a large signal increase during the Complex task and the 3 Hz task. The Complex task required additional motor and cognitive demands such as attention, decision on the forthcoming movement (selection of which finger to move) and working memory. The 3 Hz scale task required increased subject's attention. These results suggest that these areas were recruited when the motor task involved higher-order aspects of motor control. Electrophysiological studies in primates have shown that neurons in rostral parts of the striatum, including the caudate nucleus, were activated during tasks which required preparatory, working memory, early learning of complex movement sequences or reward components (Hikosaka *et al.*, 1989a,b; Kermadi *et al.*, 1993; Miyachi *et al.*, 1997; Hollerman *et al.*, 1998; Kawagoe *et al.*, 2004). Miyashi *et al.* (1997) reported that neurons which were more active during new sequences were located rostral to neurons active during learned sequences. In humans, the caudate nucleus was activated in tasks requiring preparation and selection of a sequence of movements based on information stored in working memory (Pochon *et al.*, 2001), new learning (Jueptner *et al.*, 1997a; Toni *et al.*, 1998) and planning (Dagher *et al.*, 1999).

In the globus pallidus, electrophysiological studies in monkeys have also shown that neurons active during motor tasks with cognitive components (remembered sequence task) were located dorsal and medial to GP neurons with motor related activities (Middleton and Strick, 2000), in line with the present results. Similarly, activation in the human thalamus was located in the ventral and anterior parts of the thalamus during learning of movement sequences, as shown previously (Jueptner *et al.*, 1997a).

Distinct Territories in the Basal Ganglia

The three activation patterns were observed in regions closely corresponding to the sensorimotor, premotor and prefrontal basal ganglia circuits described in non-human primates (Kunzle, 1975; Selemon and Goldman-Rakic, 1985; Yeterian and Pandya, 1991; Inase *et al.*, 1999; Middleton and Strick, 2000) and more recently in humans (Lehéricy *et al.*, 2004). In the globus pallidus of monkeys, the sensorimotor territory was located in the middle region of the structure, between the lateral premotor (ventral) and the medial premotor (mid-dorsal) areas, while the associative territory occupied more dorsomedial and rostral parts (Middleton and Strick, 2000; Kelly and Strick, 2004). The STN also includes a sensorimotor territory (dorsolaterally), distinct from an associative (ventromedially) and a limbic (medial tip) territory (Nauta and Cole, 1978; Carpenter *et al.*, 1981; Nakano *et al.*, 1990; Kelly and Strick, 2004). In the thalamus, the Vim and Vc nuclei receive cerebellar and somatosensory afferents, respectively, and the VA/VL nuclei of the thalamus receive associative and pallidal afferents (Hirai and Jones, 1989).

STN Activation

STN patterns shown in Figures 3 and 4 suggest that activation during the non-sequential Simple task extended toward the dorsal sensorimotor part of the STN, whereas activation during the sequential tasks extended toward larger parts of the nucleus, including its associative part. The STN activation greatly increased during the most difficult tasks, when movement frequency (3 Hz Scale task) and complexity (Complex task) were high. This suggests that the STN was recruited when a more precise sequence of temporally ordered inhibition and activation of motor programs was required. A leading hypothesis of the function of the indirect pathway is that it is involved in the inhibition of competing motor programs (Penney and Young, 1983; Mitchell *et al.*, 1989; Gerfen, 1992; Mink, 1996). The STN exerts a powerful excitatory drive onto GABAergic GPi and SN pars reticulata neurons, thereby increasing thalamic inhibition. In contrast, information conveyed to the GPi through the direct pathway results in inhibition of GPi neurons and of their inhibitory influence on their thalamic targets related to the selected motor program. Activation of STN neurons via the GPe or directly by cortical inputs (Maurice *et al.*, 1999; Nambu *et al.*, 2000) would result in the opposite effect, allowing inhibition of competing motor programs. The fact that STN activation was greatly enhanced during the most difficult tasks is in line with this hypothesis.

During the Complex task, activation extended toward the SN, probably reflecting the activation of midbrain dopamine neurons. DA neurons encode reward expectation error (Schultz, 2000) and/or novelty (Redgrave *et al.*, 1999). Models of basal ganglia function proposed that basal ganglia neurons integrate cortical signals with reward error signals carried by dopamine neurons during learning (Aosaki *et al.*, 1994; Doya, 2000).

Conclusion

Using higher spatial resolution and a stereotactic brain atlas, activation was observed along the entire basal ganglia circuitry.

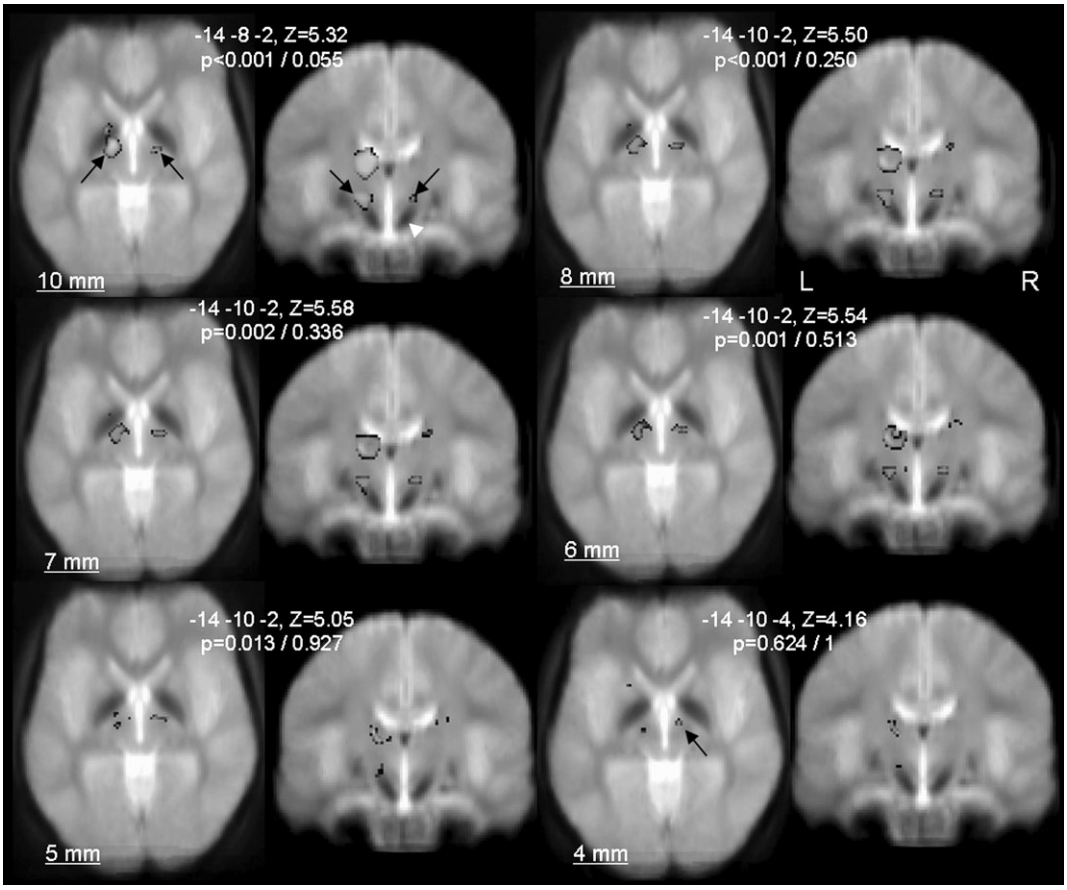

Figure 7. Effect of the size of the spatial filter on STN activation varying from 10 to 4 mm width at half maximum (from upper left to lower right, indications are Talairach coordinates of peak *Z*-score, *Z*-score, cluster/voxel corrected *P*-values in the left hemisphere). Maps are superimposed on a normalized brain EPI template. Activation in the STN is indicated by the black arrows and the SN is indicated by the white arrowhead.

Data support the hypothesis that information is processed along closed-loop cortico-basal ganglia circuits, at least for the type of movements studied. These results have important implications in movement as well as behavioral disorders (Bhatia and Marsden, 1994; Graybiel and Rauch, 2000). Recent studies in monkeys have shown that motor (dyskinesia) as well as more complex behavioral disorders such as attention deficit and stereotyped behavior, were induced by microinjections of bicuculline, a GABAergic antagonist, into the different territories of the GPe (Grabli *et al.*, 2004). It is thus expected that high resolution fMRI will help studying dysfunction of the direct and indirect circuits in basal ganglia dysfunctions.

Notes

This study was supported by grants from NIH (BTRR P41-RR08079 and RO1 EB000331), the Keck Foundation, the MIND Institute, the Human Frontiers Science Program, and the Action Concertée Incitative 2001-6503H. We thank Malgorzata Marjanska for reviewing the manuscript.

Address correspondence to Stéphane Lehéricy, CMRR, 2021 6th Street SE, Minneapolis, MN 55455, USA. Email: leherícy@cmrr.umn.edu.

References

Alexander GE, Crutcher MD (1990) Preparation for movement: neural representations of intended direction in three motor areas of the monkey. J Neurophysiol 64:133–150.

Alexander GE, DeLong MR, Strick PL (1986) Parallel organization of functionally segregated circuits linking basal ganglia and cortex. Annu Rev Neurosci 9:357–381.

Aosaki T, Graybiel AM, Kimura M (1994) Effect of the nigrostriatal dopamine system on acquired neural responses in the striatum of behaving monkeys. Science 265:412–415.

Bandettini PA, Cox RW (2000) Event-related fMRI contrast when using constant interstimulus interval: theory and experiment. Magn Reson Med 43:540–548.

Bhatia KP, Marsden CD (1994) The behavioural and motor consequences of focal lesions of the basal ganglia in man. Brain 117:859–876.

Boecker H, Dagher A, Ceballos-Baumann AO, Passingham RE, Samuel M, Friston KJ, Poline J, Dettmers C, Conrad B, Brooks DJ (1998) Role of the human rostral supplementary motor area and the basal ganglia in motor sequence control: investigations with H2 15O PET. J Neurophysiol 79:1070–1080.

Brotchie P, Iansek R, Horne MK (1991) Motor function of the monkey globus pallidus. 2. Cognitive aspects of movement and phasic neuronal activity. Brain 114:1685–1702.

Carpenter MB, Carleton SC, Keller JT, Conte P (1981) Connections of the subthalamic nucleus in the monkey. Brain Res 224:1–29.

Catalan MJ, Honda M, Weeks RA, Cohen LG, Hallett M (1998) The functional neuroanatomy of simple and complex sequential finger movements: a PET study. Brain 121:253–264.

Colebatch JG, Deiber MP, Passingham RE, Friston KJ, Frackowiak RS (1991) Regional cerebral blood flow during voluntary arm and hand movements in human subjects. J Neurophysiol 65:1392–1401.

Dagher A, Owen AM, Boecker H, Brooks DJ (1999) Mapping the network for planning: a correlational PET activation study with the Tower of London task. Brain 122:1973–1987.

DeLong MR, Crutcher MD, Georgopoulos AP (1985) Primate globus pallidus and subthalamic nucleus: functional organization. J Neurophysiol 53:530–543.
Dormont D, Ricciardi KG, Tande D, Parain K, Menuel C, Galanaud D, Navarro S, Cornu P, Agid Y, Yelnik J (2004) Is the subthalamic nucleus hypointense on T2-weighted images? A correlation study using MR imaging and stereotactic atlas data. AJNR Am J Neuroradiol 25:1516–1523.
Doya K (2000) Complementary roles of basal ganglia and cerebellum in learning and motor control. Curr Opin Neurobiol 10:732–739.
Friston KJ, Ashburner J, Poline JB, Frith CD, Heather JD, Frackowiak RS (1995) Spatial registration and normalisation of images. Hum Brain Mapp 2:165–189.
Georgopoulos AP, DeLong MR, Crutcher MD (1983) Relations between parameters of step-tracking movements and single cell discharge in the globus pallidus and subthalamic nucleus of the behaving monkey. J Neurosci 3:1586–1598.
Gerardin E, Lehéricy S, Pochon JB, Tezenas du Montcel S, Mangin JF, Poupon F, Agid Y, Le Bihan D, Marsault C (2003) Foot, hand, face and eye representation in the human striatum. Cereb Cortex 13:162–169.
Gerardin E, Pochon JB, Poline JB, Tremblay L, Van De Moortele PF, Levy R, Dubois B, Le Bihan D, Lehéricy S (2004) Distinct striatal regions support movement selection, preparation, and execution. Neuroreport 15:2327–2331.
Gerfen CR (1992) The neostriatal mosaic: multiple levels of compartmental organization in the basal ganglia. Annu Rev Neurosci 15:285–320.
Gordon AM, Lee JH, Flament D, Ugurbil K, Ebner TJ (1998) Functional magnetic resonance imaging of motor, sensory, and posterior parietal cortical areas during performance of sequential typing movements. Exp Brain Res 121:153–166.
Grabli D, McCairn K, Hirsch EC, Agid Y, Feger J, Francois C, Tremblay L (2004) Behavioural disorders induced by external globus pallidus dysfunction in primates. I. Behavioural study. Brain 127:2039–2054.
Graybiel AM, Rauch SL (2000) Toward a neurobiology of obsessive–compulsive disorder. Neuron 28:343–347.
Harrington DL, Rao SM, Haaland KY, Bobholz JA, Mayer AR, Binderx JR, Cox RW (2000) Specialized neural systems underlying representations of sequential movements. J Cogn Neurosci 12:56–77.
Haslinger B, Erhard P, Weilke F, Ceballos-Baumann AO, Bartenstein P, Grafin von Einsiedel H, Schwaiger M, Conrad B, Boecker H (2002) The role of lateral premotor–cerebellar–parietal circuits in motor sequence control: a parametric fMRI study. Brain Res Cogn Brain Res 13:159–168.
Hikosaka O, Sakamoto M, Usui S (1989a) Functional properties of monkey caudate neurons. III. Activities related to expectation of target and reward. J Neurophysiol 61:814–832.
Hikosaka O, Sakamoto M, Usui S (1989b) Functional properties of monkey caudate neurons. I. Activities related to saccadic eye movements. J Neurophysiol 61:780–798.
Hirai T, Jones EG (1989) A new parcellation of the human thalamus on the basis of histochemical staining. Brain Res Brain Res Rev 14:1–34.
Hlustik P, Solodkin A, Gullapalli RP, Noll DC, Small SL (2001) Somatotopy in human primary motor and somatosensory hand representations revisited. Cereb Cortex 11:312–321.
Hollerman JR, Tremblay L, Schultz W (1998) Influence of reward expectation on behavior-related neuronal activity in primate striatum. J Neurophysiol 80:947–963.
Inase M, Tokuno H, Nambu A, Akazawa T, Takada M (1999) Corticostriatal and corticosubthalamic input zones from the presupplementary motor area in the macaque monkey: comparison with the input zones from the supplementary motor area. Brain Res 833:191–201.
Jenkins IH, Brooks DJ, Nixon PD, Frackowiak RS, Passingham RE (1994) Motor sequence learning: a study with positron emission tomography. J Neurosci 14:3775–3790.
Jenkins IH, Passingham RE, Brooks DJ (1997) The effect of movement frequency on cerebral activation: a positron emission tomography study. J Neurol Sci 151:195–205.
Jueptner M, Frith CD, Brooks DJ, Frackowiak RS, Passingham RE (1997a) Anatomy of motor learning. II. Subcortical structures and learning by trial and error. J Neurophysiol 77:1325–1337.
Jueptner M, Stephan KM, Frith CD, Brooks DJ, Frackowiak RS, Passingham RE (1997b) Anatomy of motor learning. I. Frontal cortex and attention to action. J Neurophysiol 77:1313–1324.
Karachi C, Francois C, Parain K, Bardinet E, Tande D, Hirsch E, Yelnik J (2002) Three-dimensional cartography of functional territories in the human striatopallidal complex by using calbindin immunoreactivity. J Comp Neurol 450:122–134.
Kawagoe R, Takikawa Y, Hikosaka O (2004) Reward-predicting activity of dopamine and caudate neurons — a possible mechanism of motivational control of saccadic eye movement. J Neurophysiol 91:1013–1024.
Kawashima R, Inoue K, Sugiura M, Okada K, Ogawa A, Fukuda H (1999) A positron emission tomography study of self-paced finger movements at different frequencies. Neuroscience 92:107–112.
Kelly RM, Strick PL (2004) Macro-architecture of basal ganglia loops with the cerebral cortex: use of rabies virus to reveal multisynaptic circuits. Prog Brain Res 143:449–459.
Kermadi I, Jurquet Y, Arzi M, Joseph JP (1993) Neural activity in the caudate nucleus of monkeys during spatial sequencing. Exp Brain Res 94:352–356.
Kimura M (1990) Behaviorally contingent property of movement-related activity of the primate putamen. J Neurophysiol 63:1277–1296.
Kimura M (1992) Behavioral modulation of sensory responses of primate putamen neurons. Brain Res 578:204–214.
Krack P, Batir A, Van Blercom N, Chabardes S, Fraix V, Ardouin C, Koudsie A, Limousin PD, Benazzouz A, LeBas JF, Benabid AL, Pollak P (2003) Five-year follow-up of bilateral stimulation of the subthalamic nucleus in advanced Parkinson's disease. N Engl J Med 349:1925–1934.
Kruggel F, von Cramon DY, Descombes X (1999) Comparison of filtering methods for fMRI datasets. Neuroimage 10:530–543.
Kunzle H (1975) Bilateral projections from precentral motor cortex to the putamen and other parts of the basal ganglia. An autoradiographic study in *Macaca fascicularis*. Brain Res 88:195–209.
Lehéricy S, van de Moortele PF, Lobel E, Paradis AL, Vidailhet M, Frouin V, Neveu P, Agid Y, Marsault C, Le Bihan D (1998) Somatotopical organization of striatal activation during finger and toe movement: a 3-T functional magnetic resonance imaging study. Ann Neurol 44:398–404.
Lehéricy S, Ducros M, Van De Moortele PF, Francois C, Thivard L, Poupon C, Swindale N, Ugurbil K, Kim DS (2004) Diffusion tensor fiber tracking shows distinct corticostriatal circuits in humans. Ann Neurol 55:522–529.
Maillard L, Ishii K, Bushara K, Waldvogel D, Schulman AE, Hallett M (2000) Mapping the basal ganglia: fMRI evidence for somatotopic representation of face, hand, and foot. Neurology 55:377–383.
Maurice N, Deniau JM, Glowinski J, Thierry AM (1999) Relationships between the prefrontal cortex and the basal ganglia in the rat: physiology of the cortico-nigral circuits. J Neurosci 19:4674–4681.
Middleton FA, Strick PL (2000) Basal ganglia and cerebellar loops: motor and cognitive circuits. Brain Res Brain Res Rev 31:236–250.
Mink JW (1996) The basal ganglia: focused selection and inhibition of competing motor programs. Progr Neurobiol 50:381–425.
Mitchell IJ, Jackson A, Sambrook MA, Crossman AR (1989) The role of the subthalamic nucleus in experimental chorea. Evidence from 2-deoxyglucose metabolic mapping and horseradish peroxidase tracing studies. Brain 112:1533–1548.
Miyachi S, Hikosaka O, Miyashita K, Karadi Z, Rand MK (1997) Differential roles of monkey striatum in learning of sequential hand movement. Exp Brain Res 115:1–5.
Morel A, Magnin M, Jeanmonod D (1997) Multiarchitectonic and stereotactic atlas of the human thalamus. J Comp Neurol 387:588–630.
Mushiake H, Strick PL (1995) Pallidal neuron activity during sequential arm movements. J Neurophysiol 74:2754–2758.
Mushiake H, Inase M, Tanji J (1991) Neuronal activity in the primate premotor, supplementary, and precentral motor cortex during visually guided and internally determined sequential movements. J Neurophysiol 66:705–718.
Nakano K, Hasegawa Y, Tokushige A, Nakagawa S, Kayahara T, Mizuno N (1990) Topographical projections from the thalamus, subthalamic

nucleus and pedunculopontine tegmental nucleus to the striatum in the Japanese monkey, *Macaca fuscata*. Brain Res 537:54–68.
Nambu A, Tokuno H, Hamada I, Kita H, Imanishi M, Akazawa T, Ikeuchi Y, Hasegawa N (2000) Excitatory cortical inputs to pallidal neurons via the subthalamic nucleus in the monkey. J Neurophysiol 84:289–300.
Nauta HJ, Cole M (1978) Efferent projections of the subthalamic nucleus: an autoradiographic study in monkey and cat. J Comp Neurol 180:1–16.
Orgogozo JM, Larsen B (1979) Activation of the supplementary motor area during voluntary movement in man suggests it works as a supramotor area. Science 206:847–850.
Penney JB Jr, Young AB (1983) Speculations on the functional anatomy of basal ganglia disorders. Annu Rev Neurosci 6:73–94.
Penney JB Jr, Young AB (1986) Striatal inhomogeneities and basal ganglia function. Mov Disord 1:3–15.
Percheron G, Francois C, Talbi B, Yelnik J, Fenelon G (1996) The primate motor thalamus. Brain Res Brain Res Rev 22:93–181.
Pochon JB, Levy R, Poline JB, Crozier S, Lehéricy S, Pillon B, Deweer B, Le Bihan D, Dubois B (2001) The role of dorsolateral prefrontal cortex in the preparation of forthcoming actions: an fMRI study. Cereb Cortex 11:260–266.
Poline JB, Mazoyer BM (1994) Enhanced detection in brain activation maps using a multifiltering approach. J Cereb Blood Flow Metab 14:639–642.
Rao SM, Binder JR, Bandettini PA, Hammeke TA, Yetkin FZ, Jesmanowicz A, Lisk LM, Morris GL, Mueller WM, Estkowski LD, Wong EC, Haughton VM, Hyde JS. (1993) Functional magnetic resonance imaging of complex human movements. Neurology 43:2311–2318.
Rao SM, Bandettini PA, Binder JR, Bobholz JA, Hammeke TA, Stein EA, Hyde JS (1996) Relationship between finger movement rate and functional magnetic resonance signal change in human primary motor cortex. J Cereb Blood Flow Metab 16:1250–1254.
Redgrave P, Prescott TJ, Gurney K (1999) Is the short-latency dopamine response too short to signal reward error? Trends Neurosci 22:146–151.
Roland PE, Meyer E, Shibasaki T, Yamamoto YL, Thompson CJ (1982) Regional cerebral blood flow changes in cortex and basal ganglia during voluntary movements in normal human volunteers. J Neurophysiol 48:467–480.
Romo R, Scarnati E, Schultz W (1992) Role of primate basal ganglia and frontal cortex in the internal generation of movements. II. Movement-related activity in the anterior striatum. Exp Brain Res 91:385–395.
Rowe JB, Toni I, Josephs O, Frackowiak RS, Passingham RE (2000) The prefrontal cortex: response selection or maintenance within working memory? Science 288:1656–1660.
Saad ZS, Ropella KM, DeYoe EA, Bandettini PA (2003) The spatial extent of the BOLD response. Neuroimage 19:132–144.
Sadato N, Campbell G, Ibanez V, Deiber M, Hallett M (1996a) Complexity affects regional cerebral blood flow change during sequential finger movements. J Neurosci 16:2691–2700.
Sadato N, Ibanez V, Deiber MP, Campbell G, Leonardo M, Hallett M (1996b) Frequency-dependent changes of regional cerebral blood flow during finger movements. J Cereb Blood Flow Metab 16:23–33.
Sadato N, Ibanez V, Campbell G, Deiber MP, Le Bihan D, Hallett M (1997) Frequency-dependent changes of regional cerebral blood flow during finger movements: functional MRI compared with PET. J Cereb Blood Flow Metab 17:670–679.
Schultz W (2000) Multiple reward signals in the brain. Nat Rev Neurosci 1:199–207.
Schultz W, Romo R (1992) Role of primate basal ganglia and frontal cortex in the internal generation of movements. I. Preparatory activity in the anterior striatum. Exp Brain Res 91:363–384.
Schultz W, Tremblay L, Hollerman JR (2000) Reward processing in primate orbitofrontal cortex and basal ganglia. Cereb Cortex 10:272–284.
Selemon LD, Goldman-Rakic PS (1985) Longitudinal topography and interdigitation of corticostriatal projections in the rhesus monkey. J Neurosci 5:776–794.
Shibasaki H, Sadato N, Lyshkow H, Yonekura Y, Honda M, Nagamine T, Suwazono S, Magata Y, Ikeda A, Miyazaki M (1993) Both primary motor cortex and supplementary motor area play an important role in complex finger movement. Brain 116:1387–1398.
Talairach J, Tournoux P (1988) Co-planar stereotaxic atlas of the human brain. Stuttgart: Georg Thieme-Verlag.
Toni I, Krams M, Turner R, Passingham RE (1998) The time course of changes during motor sequence learning: a whole- brain fMRI study. Neuroimage 8:50–61.
Wexler BE, Fulbright RK, Lacadie CM, Skudlarski P, Kelz MB, Constable RT, Gore JC (1997) An fMRI study of the human cortical motor system response to increasing functional demands. Magn Reson Imaging 15:385–396.
White T, O'Leary D, Magnotta V, Arndt S, Flaum M, Andreasen NC (2001) Anatomic and functional variability: the effects of filter size in group fMRI data analysis. Neuroimage 13:577–588.
Wichmann T, Bergman H, DeLong MR (1994) The primate subthalamic nucleus. I. Functional properties in intact animals. J Neurophysiol 72:494–506.
Worsley KJ, Marrett S, Neelin P, Vandal AC, Friston KJ, Evans AC (1996) A unified statistical approach for determining significant signals in images of cerebral activation. Human Brain Mapping 4:58–73.
Wu T, Kansaku K, Hallett M (2004) How self-initiated memorized movements become automatic: a functional MRI study. J Neurophysiol 91:1690–1698.
Yelnik J, Bardinet E, Dormont D, François C, Tandé D, Parain C, Malandain G, Ayache N, Hirsch E, Agid Y (2003) Delineation of the basal ganglia in MR images of patients by automatic registration of a multimodal atlas based on histological and MR data. Neuroimage 99(S9):S48.
Yeterian EH, Pandya DN (1991) Prefrontostriatal connections in relation to cortical architectonic organization in rhesus monkeys. J Comp Neurol 312:43–67.